

Convective transitions induced by a varying aspect ratio

E. Knobloch

Physics Department, University of California, Berkeley, Berkeley, California 94720

J. Guckenheimer

University of California, Santa Cruz, Santa Cruz, California 95064

(Received 21 May 1982)

The Rayleigh number for convective instability of a horizontal layer of fluid to two-dimensional disturbances depends on the wavelength of the disturbance. In a finite rectangular domain with stress-free boundaries, there are critical lengths at which instability to two different sets of rolls occurs simultaneously. This paper gives a nonlinear analysis of this multiple-bifurcation problem. We present a complete characterization of the transitions which occur for lengths near critical. For small values of the Prandtl number the transition between the two sets of rolls occurs via a new type of solution which is represented by the superposition of the two sets of rolls with comparable amplitude. For higher Prandtl numbers the transition is an abrupt one, and is accompanied by hysteresis.

I. INTRODUCTION

Recent experimental results¹ on convection in liquid He in a box of finite size have revealed an unexpectedly rich variety of behavior. In particular, the transition in the nonlinear regime between different numbers of convection rolls can now be investigated by doing experiments in boxes of appropriately chosen sizes. The experiments on the transition from 3 rolls to 2 rolls as the Rayleigh number is increased have revealed the possibility of a mixed-mode transition, as well as more complicated oscillatory behavior between the two different convection states. The present paper describes a calculation that shows that the mixed-mode transition is characteristic of low-Prandtl-number fluids (such as helium), but that an abrupt transition involving hysteresis is to be expected in higher-Prandtl-number fluids. The critical Prandtl number dividing these two possibilities is close to that of liquid He. By varying the basic temperature of the system (and hence the Prandtl number) it might be possible to realize both kinds of transitions.

The classical analysis of a two-dimensional Boussinesq convection in a horizontally infinite layer with stress-free boundary conditions at the top and bottom shows that, as the Rayleigh number is increased, convection begins as rolls whose aspect ratio is $\sqrt{2}$. In the present problem, we are interested in examining the effects of free vertical boundaries placed as $x=0, \lambda$. When the height of the fluid is normalized to 1 and λ is not a multiple of $\sqrt{2}$, an integral number of rolls of aspect ratio $\sqrt{2}$ does not fit the box, and the first set of rolls must have an as-

pect ratio different from $\sqrt{2}$. We are interested in studying both how the aspect ratio of the rolls depends on the width λ of the box and, given λ , how it depends on the applied Rayleigh number. This problem can be studied using a bifurcation analysis. Classical perturbation techniques require the selection of a distinguished parameter that is to be varied while the remaining ones remain fixed. In this paper we use a new method of analysis²⁻⁴ which does not require the selection of such a distinguished parameter and in which a small parameter is introduced naturally in terms of a distance from a multiple bifurcation. Since the neutral curve of Rayleigh numbers for rolls of varying aspect ratios has a minimum at $\sqrt{2}$, it follows that there will be certain critical lengths $\lambda_c(k)$ at which the smallest allowed critical Rayleigh number occurs at two wave numbers $k, k+1$ with $\lambda/k+1 < \sqrt{2} < \lambda/k$. At $\lambda=\lambda_c(k)$, a multiple bifurcation from the conductive solution occurs. In this paper we determine finite-amplitude motions which occur for widths that are close to these special values of λ . The method we use, sometimes called the method of normal forms,²⁻⁴ takes full advantage of the symmetry properties of the underlying system. Moreover, the center manifold theorem⁵ provides a justification for the reduction of the bifurcation problem to a two-dimensional system of ordinary differential equations. In the present case, we compute cubic nonlinearities in the normal-form equations. By including all the modes which contribute to these cubic terms and doing a stability analysis of the resulting two-dimensional system, we obtain rigorous approximations to all of the stable steady solutions which

occur near the multiple bifurcation. In addition, we conclude that with the boundary conditions used here all solutions tend to steady-state solutions in this regime.

For systems with a large aspect ratio λ , one can adopt an alternative viewpoint based upon the techniques of Newell and Whitehead.⁶ These authors examine modulated wave trains in an infinite layer at values of the Rayleigh number slightly larger than the critical Rayleigh number R_0 for rolls of aspect ratio $\sqrt{2}$. Their analysis has been extended to the case of rigid sidewalls by Cross *et al.*⁷ In this approach, one considers the effects of sidewalls on the allowed solution for the infinite problem with $R > R_0$ fixed. Our approach differs in that we fix the width of the box λ and then increase the Rayleigh number through the *corresponding* critical Rayleigh number.

The effects of sidewalls on convection rolls have been studied before,⁷⁻¹⁴ but with particular attention paid to the bifurcation structure that arises as a result of symmetry breaking owing to heat leakage from the sides. Hall and Walton¹¹ did, however, also consider the effects of changing the box width, although with different boundary conditions from those used here and only one value of the Prandtl number. Kidachi¹³ has studied the 2-roll to 1-roll transition using modified perturbation theory, and obtained results that are in qualitative agreement with ours. Issues similar to those addressed in this paper also arise in studies of the effect on the number of Taylor vortices of varying the height of the fluid in a Taylor apparatus.^{15,16}

The formulation of the problem and the results of our calculations are presented in Sec. II, followed by some brief conclusions in Sec. III. The mathematical details are contained in the Appendix.

II. DESCRIPTION OF THE PROBLEM

Two-dimensional Boussinesq convection in a box $\{(x,z): 0 < x < \lambda h, 0 < z < h\}$ is described by the equations

$$\rho_0 \left[\frac{\partial \vec{u}}{\partial t} + \vec{u} \cdot \nabla \vec{u} \right] = -\vec{\nabla} p' + (\rho - \rho_0) \vec{g} + \rho_0 \nu \nabla^2 \vec{u}, \quad (1)$$

$$\vec{\nabla} \cdot \vec{u} = 0, \quad (2)$$

$$\frac{\partial T}{\partial t} + \vec{u} \cdot \vec{\nabla} T = \kappa \nabla^2 T, \quad (3)$$

where $\vec{u}(x,z,t)$ and $T(x,z,t)$ are the velocity and temperature fields, ρ is the density ($\rho = \rho_0$ when $T = T_0$), and p' the perturbation pressure. The constants ν and κ are, respectively, the kinematic viscosity and

the thermal conductivity, and the acceleration due to gravity \vec{g} is taken to act downwards in the negative z direction. The density change arising from a temperature change is given by

$$\rho - \rho_0 = -\alpha \rho_0 (T - T_0), \quad (4)$$

and is assumed to be negligible except when it couples to the gravitational term to provide the buoyancy forces that drive the convection.

As usual it is convenient to define $\theta(x,z,t)$, a suitably nondimensionalized departure of the temperature from the linear distribution present in the absence of convection, by

$$T - T_0 = \Delta T [1 - z + \theta(x,z,t)], \quad (5)$$

and to introduce a nondimensionalized stream function $\psi(x,z,t)$ by

$$\vec{u} = (\kappa/h) \vec{\nabla} \times (0, \psi, 0). \quad (6)$$

In Eqs. (5) and (6) the lengths are measured in units of h , and time in units of the thermal conduction time. On taking the curl of Eq. (1), we obtain the nondimensionalized equations of motion:

$$\frac{1}{\sigma} [\partial_t \nabla^2 \psi + J(\psi, \nabla^2 \psi)] = R \partial_x \theta + \nabla^4 \psi, \quad (7)$$

$$\partial_t \theta + J(\psi, \theta) = \partial_x \psi + \nabla^2 \theta, \quad (8)$$

where $J(f,g) = f_x g_z - f_z g_x$. Here R is the Rayleigh number and is a nondimensionalized measure of the temperature difference ΔT imposed across the fluid:

$$R = \frac{g \alpha \Delta T h^3}{\kappa \nu}. \quad (9)$$

The Prandtl number σ is given by

$$\sigma = \nu / \kappa. \quad (10)$$

A complete specification of the problem requires a choice of boundary conditions. For illustrative purposes we adopt here the simplest boundary conditions, with the temperature fixed at the top and bottom, no sideways heat flux, and no tangential viscous stresses. Thus we demand that

$$\psi = \psi_{zz} = \theta_z = 0 \quad \text{for } z = 0, 1, \quad (11a)$$

$$\psi = \psi_{xx} = \theta_x = 0 \quad \text{for } x = 0, \lambda. \quad (11b)$$

These boundary conditions have the advantage that the eigenfunctions of the linear problem are sines and cosines.

Equations (7) and (8) admit the trivial conductive solution $\psi = \theta = 0$ for all values of R . This solution loses stability to exponentially growing solutions of the form

$$\psi \propto e^{st} \sin(k\pi x / \lambda) \sin(\pi z)$$

when R exceeds

$$R_0(k) = \frac{\pi^4 \lambda^2}{k^2} \left[1 + \frac{k^2}{\lambda^2} \right]^3. \quad (12)$$

In an infinite layer there is a particular mode, $k/\lambda = 2^{-1/2}$, that first becomes unstable. In general, however, an integral number of cells of this wavelength will not fit into a box of width λ . Since the neutral curve $R = R_0(k)$ is concave upwards, it is possible in this case to adjust the width so that when the conductive solution loses stability, two modes,

with horizontal wave numbers k and $k+1$, set in simultaneously, with the corresponding wavelengths the first integral wavelengths to fit into the box (see Fig. 1).

For this choice of λ , $\lambda = \lambda_c(k)$, we have that $R_0(k) = R_0(k+1) \equiv R_c(k)$, and the eigenvalue $s = 0$ has multiplicity 2. In this paper we are interested in computing the dynamics for parameter values close to the critical value, and owing to the symmetries of the problem, we have to go to third order in $(\lambda - \lambda_c)^{1/2}$ and $(R - R_c)^{1/2}$. The modes that contribute to this order are given by

$$\begin{aligned} \psi(x, z, t) = & \{ a_k(t) \sin(k\pi x / \lambda) + a_{k+1}(t) \sin[(k+1)\pi x / \lambda] \} \sin(\pi z) \\ & + \{ a_{2k+1}(t) \sin[(2k+1)\pi x / \lambda] + a_1(t) \sin(\pi x / \lambda) \} \sin(2\pi z), \end{aligned} \quad (13)$$

$$\begin{aligned} \theta(x, z, t) = & \{ b_k(t) \cos(k\pi x / \lambda) + b_{k+1}(t) \cos[(k+1)\pi x / \lambda] \} \sin(\pi z) \\ & + \{ b_{2k+1}(t) \cos[(2k+1)\pi x / \lambda] + b_1(t) \cos(\pi x / \lambda) + c(t) \} \sin(2\pi z). \end{aligned} \quad (14)$$

The above choice of modes can also be justified using an amplitude expansion. Substituting these expressions into Eqs. (7) and (8) and neglecting higher-order terms, we find that the modal amplitudes satisfy the nine equations

$$a'_k + \frac{\pi^2}{4\lambda p_k} [(2k+1)(p_1 - p_{k+1})a_{k+1}a_1 - (p_{2k+1} - p_{k+1})a_{k+1}a_{2k+1}] = \sigma R \frac{k\pi}{\lambda p_k} b_k - \sigma p_k a_k, \quad (15a)$$

$$a'_{k+1} + \frac{\pi^2}{4\lambda p_{k+1}} [-(2k+1)(p_1 - p_k)a_k a_1 + (p_{2k+1} - p_k)a_k a_{2k+1}] = \sigma R \frac{(k+1)\pi}{\lambda p_{k+1}} b_{k+1} - \sigma p_{k+1} a_{k+1}, \quad (15b)$$

$$a'_{2k+1} + \frac{\pi^2}{4\lambda} \left[\frac{p_k - p_{k+1}}{p_{2k+1}} \right] a_k a_{k+1} = \sigma R \frac{(2k+1)\pi}{\lambda p_{2k+1}} b_{2k+1} - \sigma p_{2k+1} a_{2k+1}, \quad (15c)$$

$$a'_1 + \frac{\pi^2}{4\lambda} (2k+1) \left[\frac{p_{k+1} - p_k}{p_1} \right] a_k a_{k+1} = \sigma R \frac{\pi}{\lambda p_1} b_1 - \sigma p_1 a_1, \quad (15d)$$

$$b'_k - \frac{\pi^2}{4\lambda} [4ka_k c + a_{k+1}b_{2k+1} + (2k+1)a_{k+1}b_1 + a_{2k+1}b_{k+1} + (2k+1)a_1b_{k+1}] = \frac{k\pi}{\lambda} a_k - p_k b_k, \quad (15e)$$

$$\begin{aligned} b'_{k+1} + \frac{\pi^2}{4\lambda} [-4(k+1)a_{k+1}c + a_k b_{2k+1} - (2k+1)a_k b_1 + a_{2k+1}b_k + (2k+1)a_1 b_k] \\ = \frac{(k+1)\pi}{\lambda} a_{k+1} - p_{k+1} b_{k+1}, \end{aligned} \quad (15f)$$

$$b'_{2k+1} + \frac{\pi^2}{4\lambda} (-a_k b_{k+1} + a_{k+1} b_k) = \frac{(2k+1)\pi}{\lambda} a_{2k+1} - p_{2k+1} b_{2k+1}, \quad (15g)$$

$$b'_1 + \frac{\pi^2}{4\lambda} (2k+1)(a_k b_{k+1} + a_{k+1} b_k) = \frac{\pi a_1}{\lambda} - p_1 b_1, \quad (15h)$$

$$c' + \frac{\pi^2}{2\lambda} [ka_k b_k + (k+1)a_{k+1} b_{k+1}] = -4\pi^2 c, \quad (15i)$$

where

$$p_1 = \frac{\pi^2}{\lambda^2} + 4\pi^2, \quad p_k = \frac{k^2 \pi^2}{\lambda^2} + \pi^2, \quad p_{k+1} = \frac{(k+1)^2 \pi^2}{\lambda^2} + \pi^2, \quad p_{2k+1} = \frac{(2k+1)^2 \pi^2}{\lambda^2} + 4\pi^2. \quad (16)$$

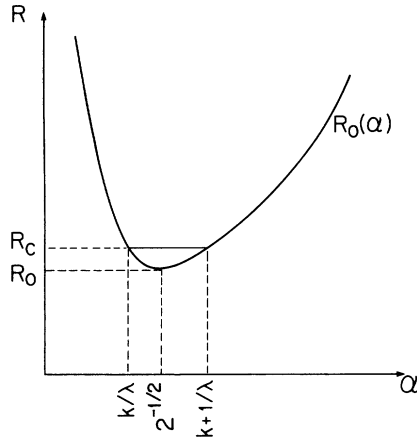


FIG. 1. Sketch of the neutral curve $R_0(\alpha)$, indicating the points of multiple bifurcation.

Equations (15) are the basic equations of this paper. By construction, when $\lambda = \lambda_c$, $R = R_c$ the linearized problem has two zero eigenvalues, the remainder having negative real parts. It follows, therefore, that in the vicinity of this bifurcation, solutions of the system (15) will contract onto a two-dimensional invariant surface on which the dynamics will be two dimensional. Methods of reducing the dynamical equations to normal (i.e., simplest) form by means of local nonlinear coordinate transformations have recently been reviewed by Guckenheimer.³ The relation of these methods to amplitude expansions has been discussed by Guckenheimer and Knobloch,⁴ who conclude that although both yield identical results, the normal-form approach is more systematic. It is therefore the approach that is adopted in the present work.

The linearized problem in the two-dimensional subspace of the zero eigenvalue has a Jordan normal form:

$$L = \begin{pmatrix} 0 & 0 \\ 0 & 0 \end{pmatrix}. \quad (17)$$

The normal form for this problem, owing to the reflectional $(Z/2Z) \times (Z/2Z)$ symmetry of the basic equations, is the same as that found for a codimen-

sion two bifurcation involving two simultaneous Hopf bifurcations with irrationally related frequencies.³ The calculation of the appropriate cases for this problem is given in detail in the Appendix. The result is summarized in the following equations:

$$a'_k = -\frac{\sigma\pi^2}{(\sigma+1)16\lambda_c^2} (2k^2 a_k^2 + B a_{k+1}^2) a_k + \mu_k a_k, \quad (18)$$

$$a'_{k+1} = \frac{-\sigma\pi^2}{(\sigma+1)16\lambda_c^2} [C a_k^2 + 2(k+1)^2 a_{k+1}^2] a_{k+1} + \mu_{k+1} a_{k+1}. \quad (19)$$

The coefficients B, C, μ_k, μ_{k+1} are given in the Appendix. The μ_i are called unfolding parameters and take into account the departure of λ and R from their critical values; they vanish at the degenerate bifurcation.

We regard both λ and R as bifurcation parameters, and present bifurcation diagrams for the system in the $(\lambda - \lambda_c)^{1/2} - (R - R_c)^{1/2}$ plane. This involves a study of the dynamics represented by the normal-form equations as functions of these two variables, or equivalently as functions of μ_k and μ_{k+1} .¹⁷ This is done by locating the fixed points, analyzing their stability, and using the divergence test to locate possible limit cycles. The results depend on the signs of the nonlinear terms. In the present case, the coefficients of a_k^3 , a_{k+1}^3 , and $a_k^2 a_{k+1}$ are all negative. The sign of the remaining coefficient depends both on k and on σ , and has to be determined numerically. The results are presented in Table I. Three distinct cases are possible. For small σ the coefficient of $a_k a_{k+1}^2$ is positive; as σ is increased this coefficient becomes negative, but the determinant of the coefficients remains positive. For still larger σ the determinant becomes negative. The bifurcation diagrams corresponding to these three cases are sketched in Fig. 2. We note that, for the coefficient signs obtaining in the present problem, no limit cycles are possible. This has the consequence that the normal forms obtained are structurally stable; if limit cycles were present fifth-order terms would have to be included to obtain structurally stable bifurcation diagrams.³ This is also true of the degenerate case

TABLE I. Coefficients B, C in the normal form equations. [Note: $B = \alpha_k + (\beta_k/\sigma) + (\gamma_k/\sigma^2)$, $C = \alpha_{k+1} + (\beta_{k+1}/\sigma) + (\gamma_{k+1}/\sigma^2)$.]

k	$\lambda_c(k)$	α_k	β_k	γ_k	α_{k+1}	β_{k+1}	γ_{k+1}	$\sigma_c(k)$
1	2.03	10.44	-0.25	-0.75	6.78	0.47	0.62	0.30
2	3.48	27.76	-0.45	-1.14	21.47	0.68	1.02	0.22
3	4.91	53.06	-0.66	-1.54	44.17	0.89	1.43	0.19
4	6.33	86.35	-0.88	-1.95	74.88	1.11	1.84	0.17

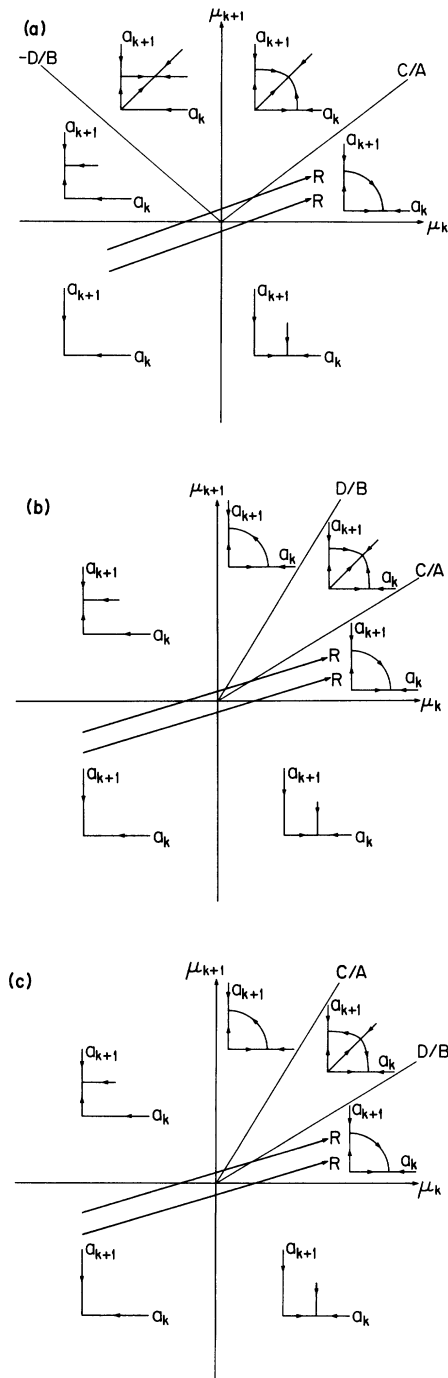


FIG. 2. Bifurcation diagrams for the normal-form equations $a'_k = -Aa_k^3 - Ba_{k+1}^2 a_k + \mu_k a_k$ and $a'_{k+1} = -Ca_k^2 a_{k+1} - Da_{k+1}^3 + \mu_{k+1} a_{k+1}$, with $A > 0$, $C > 0$, $D > 0$ and (a) $B < 0$, (b) $B > 0$, $AD - BC > 0$, and (c) $B > 0$, $AD - BC < 0$. Owing to the symmetry of the normal form only one quadrant of the $a_k - a_{k+1}$ plane is shown. The straight line, traversed in the direction shown, indicates the succession of phase portraits as the Rayleigh number is increased.

when the determinant of the coefficients vanishes. In this case a larger number of equilibrium solutions is possible. Values of $\sigma_c(k)$ for this to occur are also shown in Table I. Note that with the present boundary conditions the values of this critical Prandtl number are close to those of liquid He, in which experiments on this problem have recently been carried out.¹

In the bifurcation diagrams the heavy lines indicate the succession of phase portraits as the Rayleigh number is increased for given $\lambda - \lambda_c$. The upper line obtains in the case $\lambda > \lambda_c$, the lower when $\lambda < \lambda_c$. We see, therefore, that for $\lambda < \lambda_c$, the conductive solution always loses stability to the steady-state solution $(a_k, 0)$ as the Rayleigh number increases, and that this solution remains stable for all higher R . On the other hand if $\lambda > \lambda_c$, then the conductive solution first loses stability to mode $k + 1$. If the Prandtl number is small, then Fig. 2(a) applies, and mode $k + 1$ loses stability to a mixed mode which in turn loses stability to mode k , as the Rayleigh number increases. The bifurcation diagram for the second case, with all the coefficients negative, and the determinant of the coefficients positive, is shown in Fig. 2(b). The sequence of transitions is the same as in Fig. 2(a), except that the mixed-mode solution sets in after the critical Rayleigh number for mode k is reached. In both cases the range of Rayleigh numbers in which the mixed mode is stable is quite small. For larger values of the Prandtl number the determinant of the coefficients becomes negative, and the situation is much different. The mixed-mode solution is now unstable, and instead there is a range of Rayleigh numbers at which stable $(a_k, 0)$ and $(0, a_{k+1})$ solutions coexist. Thus, at sufficiently supercritical Rayleigh numbers, there are finite-amplitude disturbances that can cause an abrupt transition from the stable mode $k + 1$ to the stable mode k . At still higher Rayleigh numbers mode $k + 1$ loses stability, and mode k becomes the only stable solution. The above results may be summarized as follows: The preferred stable mode tends to be the mode with the longer wavelength; as $\lambda \rightarrow \infty$ this wavelength decreases monotonically to $\sqrt{2}$, the value for an infinite layer. The range of Rayleigh numbers within which the shorter mode is stable is typically small but increases with decreasing Prandtl numbers.

The limit $k, \lambda \rightarrow \infty$, with $k/\lambda = 2^{-1/2}$ and σ fixed, corresponds to allowing the box width to become infinite. Equations (18) and (19) become

$$a'_k = - \left[\frac{\sigma}{1 + \sigma} \right] \frac{\pi^2}{16} [a_k^2 + 2a_{k+1}^2 - 24(R - R_c)] a_k, \quad (20)$$

$$a'_{k+1} = - \left[\frac{\sigma}{1+\sigma} \right] \frac{\pi^2}{16} [2a_k^2 + a_{k+1}^2 - 24(R - R_c)] a_{k+1} . \quad (21)$$

In this limit the two modes k and $k+1$ are indistinguishable. We therefore take $a_{k+1}=0$. The normal-form equations then reduce to

$$a'_k = - \left[\frac{\sigma}{1+\sigma} \right] \frac{\pi^2}{16} [a_k^2 - 24(R - R_c)] a_k . \quad (22)$$

This is the usual Landau equation that describes the pitchfork bifurcation for the mode that first becomes unstable. This result may also be seen from Fig. 2 since the line along which the Rayleigh number increases is now given by $\mu_k = \mu_{k+1}$. We have thus recovered the usual results for an infinite layer. On the other hand, when λ is large but finite, and the Prandtl number σ is decreased, the normal-form equations reduce to

$$a'_k = \frac{-\sigma\pi^2}{16} [a_k^2 - Ba_{k+1}^2 - 24(R - R_c)] a_k , \quad (23)$$

$$a'_{k+1} = \frac{-\sigma\pi^2}{16} [Ba_k^2 + a_{k+1}^2 - 24(R - R_c)] a_{k+1} , \quad (24)$$

where $B = 5\sqrt{2}/24\sigma^2\lambda \gg 1$. In this case the bifurcation diagram [2(a)] still shows that the conduction solution loses stability to mode k . The approach to this solution is, however, qualitatively different from that predicted by the Landau equation (22). Strictly speaking, therefore, the two limits $\lambda \rightarrow \infty$, $\sigma \rightarrow 0$ do not commute, and the criterion that determines whether a given situation is closer to that described by Eq. (21) rather than that described by Eqs. (23) and (24) is approximately $B \leq O(1)$. To what extent this behavior is an artifact of the boundary conditions remains unclear.

We have seen that if $\lambda > \lambda_c$ and the Prandtl number is small, then in the neighborhood of the bifurcation there is a small range of values of the Rayleigh number in which a stable mixed-mode solution (a_k, a_{k+1}) is possible. Such mixed-mode solutions are characterized by the same order of magnitude of both amplitudes. These mixed modes have the interesting property that they are accompanied by large-scale motions. To see this we observe that on the invariant surface (see Appendix)

$$a_1 \propto a_k a_{k+1} . \quad (25)$$

Although the amplitude a_1 is quadratic in the amplitudes of the primary modes and therefore very small, it does show that there is a nonvanishing large-scale mode that fills the entire box. In the case of a large box, modes k and $k+1$ are essentially indistinguishable, and in this case one has rolls that are slightly tilted. This effect disappears in the limit of an infinite box.

III. DISCUSSION

We have obtained nonlinear roll solutions close to the onset of convection in a box of finite width λ , in the case where λ is close to the critical value for which the modes of wavelength λ/k and $\lambda/(k+1)$ become unstable simultaneously. We have found, for free boundaries, that if $\lambda < \lambda_c(k)$ then convection always sets in as the k mode, whereas if $\lambda > \lambda_c(k)$ then there is a narrow range of Rayleigh numbers for which mode $k+1$ is stable before it loses stability to mode k as the Rayleigh number increases. Although these results are in accord with both expectation and experiment,¹⁸ the use of the normal-form approach makes them a rigorous result for the basic fluid equations. In particular, there are no periodic, quasiperiodic, or chaotic solutions in the neighborhood of such a multiple bifurcation.

We have found that for small-Prandtl numbers, $\sigma < \sigma_c(k)$, the transition between modes $k+1$ and k occurs via a stable mixed-mode solution. The range of Rayleigh numbers over which the transition occurs is typically quite narrow, but the transition is not accompanied by hysteresis. This is in contrast to the higher-Prandtl-number case, in which the mixed-mode solution is unstable, and instead there is a range of Rayleigh numbers in which stable modes $k+1$ and k coexist. Initial conditions determine which of the two possible solutions is realized. The transition between these modes as the Rayleigh number is varied is now an abrupt one, and is accompanied by hysteresis. Such a situation is highly suggestive of the numerical results for infinite Prandtl number.¹⁹

Recently, Libchaber, and Maurer¹ have reported on an experimental study of the 3-roll to 2-roll transition in liquid He. Although they found that the transition is complicated by the presence of oscillations, some of their data are in qualitative agreement with the softer mixed-mode transition found above for $\sigma < \sigma_c(2) \approx 0.22$. In view of the proximity of this value to the Prandtl number of liquid He, $\sigma_{\text{He}} \approx 0.4-0.7$, the above calculations should be repeated for the more realistic rigid sidewalls. From symmetry considerations it follows that the normal-

form equations would remain of the forms (18) and (19), albeit with different coefficients.¹¹ Of interest is the possibility that different boundary conditions could significantly affect the Prandtl-number dependence of these coefficients. In the present problem both modes bifurcate supercritically, so that the signs of the a_k^3 or a_{k+1}^3 terms are always negative, and no new transition can occur. However, if one or the other mode were subcritical, then the corresponding stable mixed-mode solution could undergo a Hopf bifurcation.¹⁷ The limit cycle that appears disappears again in a homoclinic bifurcation as the amplitude increases. If the bifurcation were supercritical, it would manifest itself as an oscillation between two different mixed-mode states, one more nearly a pure mode $k+1$, the other more nearly a mode k . Such secondary Hopf bifurcations occur in analogous situations in magnetoconvection, convection in a rotating layer, and thermohaline convection. In the present problem, although both modes are supercritical, it is clear that a secondary Hopf bifurcation is responsible for the oscillatory transition observed by Libchaber and Maurer,¹ though apparently not at an amplitude accessible by the present analysis. Moreover, there is at present no evidence for the long periods associated with a homoclinic bifurcation. Finally, it must be emphasized that it is not clear to what extent the observed phenomena are purely two dimensional.

It is also of interest to compare our results with the analogous situation in the Taylor-Couette problem. Benjamin¹⁵ and Schaeffer¹⁶ have studied the spatial planform of the initial nonaxisymmetric flow between rotating cylinders as a function of the height of the apparatus. The usual pattern which forms in an apparatus with rigid end walls consists of an even number of Taylor vortices. Here, as in the situation we consider, there will be critical distances for the end-wall separation at which two modes become unstable simultaneously. If the coefficients of the cross terms in the normal form have the same sign and are large relative to the diagonal terms, then mixed-mode solutions do not appear in the theory, and instead the system exhibits hysteresis and parameter regimes in which two stable steady states occur. All transitions are abrupt jumps between these stable pure-mode solutions rather than the "softer" transitions involving mixed-mode solutions. Such behavior is in excellent qualitative agreement with the experimental results.¹⁵ Unfortunately, for this problem the coefficients in the normal-form equations have not actually been calculated because of the complexity of the calculations, so that the conjectured conditions on the coefficients have not been explicitly verified.

ACKNOWLEDGMENTS

We are indebted to A. Libchaber and E. Siggia for discussions, and to P. Coullet, J. Magnan, and E. Spiegel for pointing out Refs. 12–14. This work was completed as part of the 1981 Summer Program in Geophysical Fluid Dynamics at the Woods Hole Oceanographic Institution. One of us (J.G.) was supported in part by NSF Grant No. MCS 79-02002. The other (E.K.) was supported by an Alfred P. Sloan Foundation fellowship and NSF Grant No. AST 79-23243.

APPENDIX: COMPUTATION OF THE NORMAL FORM

In this appendix we explain in some detail how a system of nonlinear ordinary differential equations is reduced to normal form in the vicinity of a bifurcation point. We suppose that the equations admit the trivial fixed point 0 [cf. Eq. (15)], and note that at a bifurcation point the real parts of one or more eigenvalues of the linearized problem pass through zero. The solution trajectories contract in the eigendirections corresponding to those eigenvalues that have a negative real part, and end up on an invariant surface, called the center manifold, whose dimension equals the number of eigenvalues that pass through zero plus the number of complex pairs of eigenvalues whose real parts pass through zero. In the vicinity of the bifurcation, the dynamics of interest is therefore that associated with the zero real-part eigenvalues, and takes place on the center manifold. Mathematically, this is justified by the center manifold theorem.⁵ The central part of the reduction is therefore a computation of the center manifold and of the appropriate coordinates on the center manifold in terms of which the dynamics is as simple as possible. The background to the method and its relation to amplitude expansions are reviewed by Guckenheimer and Knobloch.⁴

In the present case the bifurcation has a two-dimensional eigenspace for the zero eigenvalue. The dynamics will therefore be two dimensional. The first stage in the reduction is to write the equations for the linear problem in Jordan normal form. We introduce new variables (\bar{a}_l, \bar{b}_l) , $l = k, k+1$, defined by

$$\begin{bmatrix} \bar{a}_l \\ \bar{b}_l \end{bmatrix} = S_l^{-1} \begin{bmatrix} a_l \\ b_l \end{bmatrix}, \quad S_l = \begin{bmatrix} 1 & 1 \\ \frac{l\pi}{\lambda p_l} & \frac{-l\pi}{\sigma \lambda p_l} \end{bmatrix}, \quad (\text{A1})$$

and write Eqs. (15a), (15e), (15b), and (15f) in the form

$$\begin{pmatrix} \bar{a}_l \\ \bar{b}_l \end{pmatrix}' = \begin{pmatrix} 0 & 0 \\ 0 & -(1+\sigma)p_l \end{pmatrix} \begin{pmatrix} \bar{a}_l \\ \bar{b}_l \end{pmatrix} + S_l^{-1} \underline{N}_l. \quad (\text{A2})$$

Here \underline{N}_l represents the nonlinear terms. The dynamics on the center manifold are associated with the modes \bar{a}_k, \bar{a}_{k+1} . The center manifold is tangential to the surface defined by

$$\bar{b}_k = \bar{b}_{k+1} = 0, \quad (\text{A3})$$

together with five other conditions involving the modes corresponding to $c, a_{2k+1}, a_1, b_{2k+1}$, and b_1 . The calculation of all these is similar, but the center manifold cannot be specified simply by setting

$$c = a_{2k+1} = a_1 = b_{2k+1} = b_1 = 0.$$

This is because the center manifold is curved and, in fact, has a quadratic tangency at the origin in these directions. The quadratic terms in the equations for \bar{a}_k, \bar{a}_{k+1} which are of the form pq , where $p = \bar{a}_k$ or \bar{a}_{k+1} and $q = c, a_{2k+1}, a, b_{2k+1}$, or b_1 , will therefore contribute cubic terms to the normal form on the center manifold.

The calculation involving mode c is typical. We suppose that, to second order, the center manifold is defined by

$$z = c + Q(\bar{a}_k, \bar{a}_{k+1}), \quad (\text{A4})$$

where

$$Q = \alpha \bar{a}_k^2 + 2\beta \bar{a}_k \bar{a}_{k+1} + \gamma \bar{a}_{k+1}^2. \quad (\text{A5})$$

Writing Eq. (15i) in terms of z, \bar{a}_k, \bar{b}_k , we obtain

$$z' = -4\pi^2 z + 4\pi Q - \frac{\pi^3}{2\lambda^2} \left[\frac{k^2}{p_k} (\bar{a}_k + \bar{b}_k) \left(\bar{a}_k - \frac{1}{\sigma} \bar{b}_k \right) + \frac{(k+1)^2}{p_{k+1}} (\bar{a}_{k+1} + \bar{b}_{k+1}) \left(\bar{a}_{k+1} - \frac{1}{\sigma} \bar{b}_{k+1} \right) \right]. \quad (\text{A6})$$

But on the center manifold (A3) holds, so that if we choose

$$\alpha = \frac{k^2 \pi}{8\lambda^2 p_k}, \quad \beta = \frac{(k+1)^2 \pi}{8\lambda^2 p_{k+1}}, \quad \gamma = 0, \quad (\text{A7})$$

we find that

$$z' = -4\pi^2 z + \dots, \quad (\text{A8})$$

where the ellipses stand for cubic terms. To second order, the center manifold is therefore given by the condition $z = 0$, or

$$c = -Q(\bar{a}_k, \bar{a}_{k+1}). \quad (\text{A9})$$

The computation for the other modes proceeds similarly. The coupled equations for (a_{2k+1}, b_{2k+1}) are first diagonalized, and written in terms of the coordinates

$$\begin{pmatrix} \bar{a}_{2k+1} \\ \bar{b}_{2k+1} \end{pmatrix} = S_{2k+1}^{-1} \begin{pmatrix} a_{2k+1} \\ b_{2k+1} \end{pmatrix}, \quad S_{2k+1} = \begin{pmatrix} 1 & 1 \\ \frac{(2k+1)\pi/\lambda}{p_{2k+1} - s_{2k+1}^1} & \frac{(2k+1)\pi/\lambda}{p_{2k+1} - s_{2k+1}^2} \end{pmatrix}, \quad (\text{A10})$$

where s_{2k+1}^1, s_{2k+1}^2 are the eigenvalues of the linear problem and satisfy

$$(s - \sigma p_{2k+1})(s - p_{2k+1}) - \sigma R \frac{(2k+1)^2 \pi^2}{\lambda^2 p_{2k+1}} = 0. \quad (\text{A11})$$

The variable z_{2k+1} is defined, analogously to (A4), to vanish on the center manifold. A straightforward calculation yields the condition

$$\bar{a}_{2k+1} = \frac{\pi^3}{4\lambda^2 s_{2k+1}^1 D_{2k+1}} \left[\left[\frac{2k+1}{p_{2k+1} - s_{2k+1}^2} \right] \left[\frac{p_{k+1} - p_k}{p_{2k+1}} \right] + \left[\frac{k}{p_k} - \frac{k+1}{p_{k+1}} \right] \right] \bar{a}_k \bar{a}_{k+1}, \quad (\text{A12})$$

with similar results for $\bar{b}_{2k+1}, \bar{a}_1, \bar{b}_1$. Here $D_{2k+1} = \det S_{2k+1}$. Note that with these values the nonlinear terms in (A2) are cubic so that (A3) is indeed the correct condition for the center manifold. No further nonlinear terms need to be taken into account for computing the cubic terms of the center manifold.

Using the results (A9), (A12), and their analogs we can now evaluate the nonlinear terms in the equations for \bar{a}_k, \bar{a}_{k+1} . These can be simplified by eliminating the eigenvalues $s_i^{1,2}$ using the characteristic equations [cf. Eq.

(A11)]. The result can be written in the form

$$\bar{a}'_k = -\frac{\sigma\pi^2}{(\sigma+1)16\lambda_c^2} \left[2k^2\bar{a}_k^2 + \left[\alpha_k + \frac{\beta_k}{\sigma} + \frac{\gamma_k}{\sigma^2} \right] \bar{a}_{k+1}^2 \right] \bar{a}_k, \quad (\text{A13})$$

$$\bar{a}'_{k+1} = -\frac{\sigma\pi^2}{(\sigma+1)16\lambda_c^2} \left[\left[\alpha_{k+1} + \frac{\beta_{k+1}}{\sigma} + \frac{\gamma_{k+1}}{\sigma^2} \right] \bar{a}_k^2 + 2(k+1)^2\bar{a}_{k+1}^2 \right] \bar{a}_{k+1}, \quad (\text{A14})$$

where

$$\alpha_k = 2(k+1)^2 \frac{p_k}{p_{k+1}} + r_1 \left[p_1^2 + \frac{p_{k+1}^2}{k+1} \right] (1+\delta) + r_{2k+1} \left[p_{2k+1}^2 + \frac{p_{k+1}^2(2k+1)}{k+1} \right] (1-\delta),$$

$$\beta_k = -r_1 \left[\left[p_1\delta + \frac{p_k}{k} \right] (p_k - p_{k+1}) + \left[\frac{p_1 - p_{k+1}}{p_k} \right] \left[\frac{p_k^2}{k} + \frac{p_{k+1}^2}{k+1} \right] \right] \\ + r_{2k+1} \left[\left[p_{2k+1}\delta + \frac{2k+1}{k} p_k \right] (p_k - p_{k+1}) + \left[\frac{p_{2k+1} - p_{k+1}}{p_k} \right] (2k+1) \left[\frac{p_k^2}{k} - \frac{p_{k+1}^2}{k+1} \right] \right],$$

$$\gamma_k = \left[\frac{p_k - p_{k+1}}{p_k} \right] [r_1 p_1 (p_1 - p_{k+1}) + r_{2k+1} p_{2k+1} (p_{2k+1} - p_{k+1})],$$

$$\alpha_{k+1} = 2k^2 \frac{p_{k+1}}{p_k} + r_1 \left[p_1^2 - \frac{p_k^2}{k} \right] (1+\delta^{-1}) + r_{2k+1} \left[p_{2k+1}^2 + \frac{p_k^2}{k} (2k+1) \right] (1-\delta^{-1}),$$

$$\beta_{k+1} = r_1 \left[\left[\frac{p_1}{\delta} - \frac{p_{k+1}}{k+1} \right] (p_k - p_{k+1}) + \left[\frac{p_1 - p_k}{p_{k+1}} \right] \left[\frac{p_k^2}{k} + \frac{p_{k+1}^2}{k+1} \right] \right] \\ - r_{2k+1} \left[\left[\frac{p_{2k+1}}{\delta} + (2k+1) \frac{p_{k+1}}{k+1} \right] (p_k - p_{k+1}) + \left[\frac{p_{2k+1} - p_k}{p_{k+1}} \right] (2k+1) \left[\frac{p_k^2}{k} - \frac{p_{k+1}^2}{k+1} \right] \right],$$

$$\gamma_{k+1} = -\left[\frac{p_k - p_{k+1}}{p_{k+1}} \right] [r_1 p_1 (p_1 - p_k) + r_{2k+1} p_{2k+1} (p_{2k+1} - p_k)],$$

with

$$r_1 = \frac{(2k+1)^2 \pi^2}{p_1^3 \left[1 - \left[\frac{1}{k} \right]^2 \left[\frac{p_k}{p_1} \right]^3 \right]}, \quad r_{2k+1} = \frac{\pi^2}{p_{2k+1}^3 \left[1 - \left[\frac{2k+1}{k} \right]^2 \left[\frac{p_k}{p_{2k+1}} \right]^3 \right]}, \quad \delta = \frac{k+1}{k} \frac{p_k}{p_{k+1}}.$$

We must consider what happens when the parameter of the problem, the width λ , differs by a small amount from the critical value $\lambda_c(k)$ at which the k and $k+1$ mode become unstable simultaneously. In this case, there will be two simple bifurcations in close succession, and the degeneracy of the bifurcation is broken. This has the effect of adding linear terms $\mu_k \bar{a}_k$ and $\mu_{k+1} \bar{a}_{k+1}$ to the right-hand sides of (A13) and (A14), respectively.

We define $\epsilon \ll 1$ by the relation

$$\lambda^2 = \lambda_c^2 (1 \pm \epsilon^2),$$

and let

$$R = R_c (1 + \mu \epsilon^2),$$

where $\mu = O(1)$, and $\lambda_c(k)$ and $R_c(k)$ are the width and Rayleigh number at which modes k and $k+1$ appear simultaneously. It follows that

$$R_l = R_c \left[1 \pm \frac{\lambda_c^2 - 2l^2}{\lambda_c^2 + l^2} \epsilon^2 + O(\epsilon^4) \right], \quad l = k, k + 1.$$

Equation (A2) then has an additional term on the right-hand side given by

$$\epsilon^2 (S_l^{-1})_c \left[\begin{array}{c} \pm \frac{\sigma \pi^2 l^2}{\lambda_c^2} R_c \frac{\sigma l}{\pi} \left[\frac{\lambda_c}{\lambda_c^2 + l^2} \right] \left[\mu \pm \frac{l^2 - \lambda_c^2}{2(l^2 + \lambda_c^2)} \right] \\ \mp \frac{\pi l}{2\lambda_c} \qquad \qquad \qquad \pm \frac{\pi^2 l^2}{\lambda_c^2} \end{array} \right] (S_l)_c \begin{bmatrix} \bar{a}_l \\ \bar{b}_l \end{bmatrix},$$

where $(S_l)_c$ is the matrix (A1) evaluated for $\lambda = \lambda_c$. After some simplification we find that

$$\mu_l = \frac{\epsilon^2 \sigma \pi^2}{(1 + \sigma) \lambda_c^2} [\pm (2l^2 - \lambda_c^2) + (l^2 + \lambda_c^2) \mu]. \quad (\text{A15})$$

Finally we note that on the center manifold $\bar{b}_k = \bar{b}_{k+1} = 0$, so that $\bar{a}_k = a_k$ and $\bar{a}_{k+1} = a_{k+1}$. The normal-form equations (A13) and (A14) can therefore be written in terms of the amplitudes a_k and a_{k+1} . With the contributions (A15) they can therefore be written in the form (19). This completes the derivation of the normal-form equations for this problem.

¹A. Libchaber and J. Maurer, in *Nonlinear Phenomena at Phase Transitions and Instabilities*, edited by T. Riste (Plenum, New York, 1981), p. 259.

²P. J. Holmes, *Physica (Utrecht)* **2D**, 449 (1981).

³J. Guckenheimer (unpublished).

⁴J. Guckenheimer and E. Knobloch (unpublished).

⁵J. E. Marsden and M. McCracken, *The Hopf Bifurcation and its Applications* (Springer, New York, 1976).

⁶A. C. Newell and J. A. Whitehead, *J. Fluid Mech.* **38**, 279 (1969).

⁷M. C. Cross, P. G. Daniels, P. C. Hohenberg, and E. D. Siggia, *Phys. Rev. Lett.* **45**, 898 (1980), and a report (unpublished).

⁸L. A. Segel, *J. Fluid Mech.* **38**, 203 (1969).

⁹P. G. Daniels, *Proc. R. Soc. London, Ser. A* **358**, 173 (1977).

¹⁰P. Hall and I. C. Walton, *Proc. R. Soc. London, Ser. A* **358**, 199 (1977).

¹¹P. Hall and I. C. Walton, *J. Fluid Mech.* **90**, 377 (1979).

¹²J.-P. Poyet, Ph.D. thesis, Astronomy Department, Columbia University (1980) (unpublished).

¹³H. Kidachi, *Prog. Theor. Phys.* **64**, 1861 (1980); **68**, 49 (1982).

¹⁴J. Coste and N. Peyraud, *Phys. Lett.* **83A**, 263 (1981).

¹⁵T. B. Benjamin, *Proc. R. Soc. London, Ser. A* **359**, 1 (1978); **A 359**, 27 (1978).

¹⁶D. Schaeffer, *Math. Proc. Cambridge Philos. Soc.* **87**, 307 (1980).

¹⁷J. P. Keener, *Stud. Appl. Math.* **55**, 187 (1976).

¹⁸R. Krishnamurti, *J. Fluid Mech.* **42**, 295 (1970).

¹⁹T. D. Foster, *J. Fluid Mech.* **37**, 81 (1969).